Draft version July 25, 2008
Preprint typeset using LaTeX style emulateapj v. 11/12/01

arXiv:0807.3985v1 [astro-ph] 25 Jul 2008

ANOMALOUS MICROWAVE EMISSION FROM THE HII REGION RCW175

C. Dickinson,[1] R. D. Davies,[2] J. R. Allison,[3] J. R. Bond,[4] S. Casassus,[5] K. Cleary,[6]
R. J. Davis,[2] M. E. Jones,[3] B. S. Mason,[7] S. T. Myers,[8] T. J. Pearson,[6] A. C. S. Readhead,[6]
J. L. Sievers,[4] A. C. Taylor,[3] M. Todorović,[2] G. J. White,[9] P. N. Wilkinson[2]

Draft version July 25, 2008

ABSTRACT

We present evidence for anomalous microwave emission in the RCW175 HII region. Motivated by 33 GHz 13′ resolution data from the Very Small Array (VSA), we observed RCW175 at 31 GHz with the Cosmic Background Imager (CBI) at a resolution of 4′. The region consists of two distinct components, G29.0-0.6 and G29.1-0.7, which are detected at high signal-to-noise ratio. The integrated flux density is 5.97 ± 0.30 Jy at 31 GHz, in good agreement with the VSA. The 31 GHz flux density is 3.28 ± 0.38 Jy (8.6σ) above the expected value from optically thin free-free emission based on lower frequency radio data and thermal dust constrained by IRAS and WMAP data. Conventional emission mechanisms such as optically thick emission from ultracompact HII regions cannot easily account for this excess. We interpret the excess as evidence for electric dipole emission from small spinning dust grains, which does provide an adequate fit to the data.

Subject headings: radio continuum: ISM — ISM: individual (RCW175) — radiation mechanisms: general

1. INTRODUCTION

In recent years there has been mounting observational evidence for a new diffuse component emitting at frequencies $\approx 10 - 60$ GHz. The anomalous microwave emission was first detected at 14 and 32 GHz by Leitch et al. (1997). Since then, a similar picture has emerged both at high latitudes (Banday et al. 2003; de Oliveira-Costa et al. 2004; Fernández-Cerezo et al. 2006; Hildebrandt et al. 2007; Bonaldi et al. 2007) and from individual Galactic sources (Casassus et al. 2004, 2006, 2007; Watson et al. 2005; Scaife et al. 2007; Dickinson et al. 2007), although negative detections have also been reported (Dickinson et al. 2006; Scaife et al. 2008). The spectral index between 20 and 40 GHz is $\alpha \approx -1.1$ (Davies et al. 2006) with some evidence of flattening at $\sim 10-15$ GHz (Leitch et al. 1997; de Oliveira-Costa et al. 2004; Hildebrandt et al. 2007). The emission appears to be very closely correlated with far-IR data suggesting a dust origin. Various emission mechanisms have been suggested, including hot ($T \sim 10^6$ K) free-free (Leitch et al. 1997), flat spectrum synchrotron (Bennett et al. 2003), spinning dust (Draine & Lazarian 1998a,b) and magnetic dust (Draine & Lazarian 1999). The overall picture is still very unclear and new data covering the range $10 - 60$ GHz are urgently needed.

RCW175 (Rodgers et al. 1960) is a diffuse HII region, which consists of a "medium brightness" optical filament (G29.1-0.7, S65) $\sim 7' \times 5'$ in extent, and a nearby compact source (G29.0-0.6), which is heavily obscured by dust. Although the filament is clearly seen in high resolution data, the compact counterpart is considerably brighter. The ionization is thought to be provided by a single B-1 II type star, which forms part of a 5-star cluster (Forbes 1989; Sharpless 1959) at a distance of 3.6 kpc.

Observations made with the Very Small Array (VSA) at 33 GHz (Watson et al. 2003; Dickinson et al. 2004) as part of a Galactic plane survey (Todorović et al., in prep.) indicate that RCW175 is anomalously bright by a factor of ≈ 2, when compared with lower frequency data. In this *Letter*, we present accurate Cosmic Background Imager (CBI) 31 GHz observations of RCW175 and make a comparison with ancillary radio/FIR data. We find that the emission at 31 GHz is significantly above what is expected from a simple model of free-free and vibrational dust emissions.

2. DATA

2.1. *31 GHz: Cosmic Background Imager*

The CBI is a $26 - 36$ GHz 13-element comounted interferometer, operated at the Chajnantor Observatory, Chile. The original CBI used 0.9 m dishes to provide high temperature sensitivity measurements on angular scales $\sim 30'-6'$ (Padin et al. 2002; Readhead et al. 2004). Recently, it has been upgraded with 1.4 m dishes (CBI2) to give increased temperature sensitivity on angular scales $\approx 4'-15'$ (Taylor et al., in prep.).

---

[1] Infrared Processing and Analysis Center, California Institute of Technology, M/S 220-6, 1200 E. California Blvd., Pasadena, CA 91125, U.S.A.
[2] Jodrell Bank Observatory, University of Manchester, Lower Withington, Macclesfield, Cheshire, SK11 9DL, U.K.
[3] Oxford Astrophysics, University of Oxford, Denys Wilkinson Building, Keble Road, Oxford, OX1 3RH, U.K.
[4] Canadian Institute for Theoretical Astrophysics, University of Toronto, Toronto, Canada.
[5] Departamento de Astronomía, Universidad de Chile, Casilla 36-D, Santiago, Chile.
[6] Chajnantor Observatory, California Institute of Technology, M/S 105-24, Pasadena, CA 91125, U.S.A.
[7] National Radio Astronomy Observatory, Green Bank, WV.
[8] National Radio Astronomy Observatory, Socorro, NM.
[9] Rutherford Appleton Laboratory, Didcot, OX11 0QX, U.K.

We observed RCW175 at RA= $18^{\rm h}46^{\rm m}40^{\rm s}$, Dec= $-03^{\rm d}46^{\rm m}00^{\rm s}$ (J2000), on 4 nights in May 2007, with a total integration time of 6 hr with CBI2. Boresight rotations of the array were used to improve the u, v-coverage. Ground spillover was removed by subtracting observations of a comparison field, 8 min later in RA, observed at the same hour angles. Jupiter was the primary amplitude/phase calibrator with absolute calibration tied to a Jupiter temperature of 146.6 ± 0.75 K at 33 GHz (Hill et al. 2008). Observations of secondary calibrators showed that the pointing was good to better than $1'$.

A uniform-weighted, CLEANed map is shown in Fig. 1. The synthesized beam is $4'.3 \times 4'.0$ and the primary beam is approximately Gaussian with FWHM $28'.2$ ($30{\rm GHz}/\nu$). Corrections for the primary beam were made directly to the CLEAN components at each frequency; the bulk of the emission fits well within the extent of the primary beam. The total flux density in the map is 6.4 Jy with a peak brightness of 1.04 Jy/beam and the noise level is 27 mJy/beam.

The CBI map detects and resolves both components in the RCW175 region. G29.0-0.6 in the west is more compact and is significantly brighter than the more diffuse G29.1-0.7 in the east. Although there is some extended emission almost all (93%) of the flux can be fitted by two Gaussian components. Note that the entire extent of RCW175 is equivalent to ≈ 13 beam areas, thus the maximum CLEAN bias is ≈ 0.35 Jy. We fitted two elliptical Gaussians plus a baseline offset using the AIPS task JMFIT. At 31 GHz we find that G29.0-0.6 has a deconvolved size $5'.4 \times 5'.1$ and integrated flux density, $S_i = 2.20$ Jy. G29.1-0.7 is $10'.0 \times 8'.2$ and $S_i = 3.76$ Jy. Simulations showed that CBI flux-loss due to the limited u, v-coverage is $\lesssim 10\%$ when fitting two Gaussians to the bulk of the emission.

2.2. *Ancillary radio/FIR data*

Table 1 lists frequencies, angular resolutions and references for the data[10] used in this *Letter* and Fig. 1 shows selected maps centered on RCW175. The radio maps from 1.4 GHz to 14.35 GHz show enhanced emission at the same location as that seen in the CBI image with the bright, more compact, hotspot in the west (G29.0-0.6) and the fainter component to the east (G29.1-0.7). For data with resolutions $\sim 4'$, the sub-components are not well separated and the bulk of the emission is confined to a region $\sim 10' \times 5'$. At these resolutions the region looks like one extended object with G29.0-0.6 dominating at one end. The higher resolution NVSS 1.4 GHz/*Spitzer* 24 μm data show the more compact G29.0-0.6 has an extent of $\approx 2'$. A filament of emission to the east (G29.1-0.7) is coincident with the filament seen in high resolution optical/IR images. There is low-level emission in the region in between, which is particularly evident in the 24 μm image.

WMAP 5-yr total-intensity maps (Hinshaw et al. 2008) covering 23-94 GHz show no significant detection of emission above the Galactic background at the location of RCW175. The 94 GHz map, at $\approx 12'.6$ resolution, is however useful for placing an upper limit on the thermal dust contribution (see §3.1).

3. FLUX DENSITY SPECTRUM

3.1. *Integrated flux density spectrum*

The integrated flux density in each map was calculated both by fitting multiple Gaussians (with baseline offset) and by integrating over a given aperture. For the interferometric data, both methods gave roughly consistent results within the errors. For total-power data, the aperture value could be over-estimated due to the background level. Moreover, a possible offset of $\sim 0.'5$ in the CBI map could result in a bias depending on the exact aperture location; an offset of $\approx 0'.5$ does appear to be visible when comparing CBI contours with the NVSS 1.4 GHz map (Fig. 1). For these reasons, we chose the Gaussian fitting method as described in §2.1.

Integrated flux densities for RCW175 and the G29.0-0.6 component are given in Table 1 and plotted in Fig. 2. Absolute calibration errors (assumed to be 10% if not known) were added in quadrature to the fitting error reported by JMFIT. We include the 33 GHz value for RCW175 from the VSA, which is in good agreement with the CBI value. The lower resolution ($\approx 13'$) VSA data meant that a single Gaussian fit was adequate and that flux loss was negligible. Since there is a correction factor of 1.53 for the primary beam at the position of RCW175, we assigned a conservative 10% error to account for any small deviations from the assumed Gaussian primary beam. An upper limit was inferred from the WMAP W-band (94 GHz) map by fitting for a parabolic baseline in the vicinity of RCW175 to account for the Galactic background, and calculating the 3σ of the residual map.

3.2. *SED fitting*

For a classical HII region, the radio/microwave spectrum consists of free-free emission at radio wavelengths and vibrational dust emission at infrared wavelengths. At the lowest radio frequencies (typically $\lesssim 1$ GHz), the free-free emission is optically thick and follows a $\alpha \approx +2$ spectrum[11]. Above the turnover frequency (typically $\sim$ 1 GHz), the emission becomes optically thin and follows a $\alpha \approx -0.1$ power-law, with very little dependence on physical conditions (Rybicki & Lightman 1979; Dickinson et al. 2003). At high frequencies (typically > 100 GHz), vibrational dust emission becomes dominant. Vibrational dust is well-represented by a modified black-body function, $\nu^{\beta+2} B(\nu, T_{\rm dust})$, where β is the dust emissivity index and $B(\nu, T_{\rm dust})$ is the black-body function for a given dust temperature, $T_{\rm dust}$.

The SED for RCW175 and the G29.0-0.6 component is shown in Fig. 2. The low frequency (< 15 GHz) data were fitted by an optically thin free-free power-law spectrum ($S \propto \nu^{\alpha}$) fixed to the theoretical value, $\alpha = -0.12$ for $T_e \approx$ 8000 K and frequencies around ~ 10 GHz. When fitting for the index we found $\alpha = -0.32 \pm 0.15$, which is consistent with this value. The infrared data (60/100 μm) were fitted by a single temperature dust component using a simple modified black-body curve, $S \propto \nu^{\beta+2} B(\nu, T_{\rm dust})$. We did not attempt to fit data at shorter wavelengths. Since there are no data points in the sub-mm ($\sim 100-1000$ GHz), the emissivity index was fixed at $\beta = +2.0$, which is typical for HII regions (e.g. Gordon (1988)). Flatter indices in the range $\beta \approx 1-2$ have been observed while the preferred value for $T_{\rm dust} \approx 30$ K is $\beta \approx +1.6$ (Dupac et al. 2003). However, the 94 GHz upper limit does not allow flatter indices than $\beta \approx 2$. The best-fitting dust temperatures were $T_{\rm dust} = 30.1 \pm 5.7$ K and $T_{\rm dust} = 37.6 \pm 6.4$ K, for RCW175 and G29.0-0.6, respectively.

---

[10] Data were downloaded from the *Skyview* website (http://skyview.gsfc.nasa.gov), the MPIfR Image Survey Sampler website (http://www.mpifr-bonn.mpg.de/survey.html), the LAMBDA website (http://lambda.gsfc.nasa.gov/) and the IRSA website (http://irsa.ipac.caltech.edu)

[11] Throughout this *Letter*, we use the spectral index convention for flux density given by $S \propto \nu^{\alpha}$.

From Fig. 2 it is clear that the ~ 30 GHz flux densities are significantly higher than the simple model can allow for. This model predicts a 31 GHz flux density for RCW175 of 2.69 ± 0.24 Jy, compared to the measured value of 5.97 ± 0.30 Jy. This corresponds to an excess over the free-free emission of 3.28 ± 0.38 Jy (8.6σ). Adopting the best-fit spectral index at low frequencies results in a larger excess at 31 GHz, although at a reduced significance level (6.4σ) due to the increased error when fitting for an additional parameter. The brighter component of G29.0-0.6 shows a similar level of excess (Fig. 2).

4. DISCUSSION

A peaked (convex) spectrum is required to produce excess emission at ~ 30 GHz without exceeding the upper limit at 94 GHz. The 3σ upper limit at 94 GHz strongly rules out a cold thermal dust component, or a flatter dust emissivity. Convex spectra can be produced by optically thick ultracompact (UC) HII regions, gigahertz-peaked spectrum (GPS) sources, or some new mechanism such as electro-dipole and magneto-dipole radiation.

UC HII regions are self-absorbed up to higher frequencies because of extremely high densities. Indeed it is possible to fit the radio data including the VSA/CBI data by including a homogenous compact HII region with angular size $\sim 1''$ and emission measure of $\sim 3 \times 10^{9}$ cm^{-6}pc. Such parameters are within observed limits (Wood & Churchwell 1989). However, the additional component produces too much flux ($\gtrsim 10$ Jy) at 94 GHz. For the same reasons, magneto-dipole radiation can also be excluded as a major contributor.

GPS sources are high redshift radio sources in which the radio jets have been highly confined and the synchrotron emission is self-absorbed. A search through the NVSS catalogue (Condon et al. 1998) revealed no bright ($\gtrsim 100$ mJy) compact radio sources in this region and no bright ($\gtrsim 20$ mJy), point-like sources appear in the NVSS 1.4 GHz map.

The anomalous emission could be due to electric dipole radiation from small rapidly spinning dust grains. If such grains have a residual dipole moment and spin at GHz frequencies, they will emit over a narrow range of frequencies. Fig. 2 shows a typical spinning dust spectrum using the model of Draine & Lazarian (1998b) for the Cold Neutral Medium (CNM), scaled to fit the VSA/CBI data. The highly peaked spectrum allows an adequate fit to the data both at ~ 10 GHz and yet consistent with the 94 GHz upper limit. We note that the appropriate model for Warm Ionized Medium (WIM) peaks at a slightly lower frequency and predicts too much flux at ~ 10 GHz. However, the models are fairly generic and allow considerable freedom in the dust parameters (Finkbeiner 2004). A similar situation is observed in the HII region G159.6-18.5 (Watson et al. 2005) and the dark cloud LDN1622 (Casassus et al. 2006).

The Draine & Lazarian (1998b) models are expressed in terms of the intensity per hydrogen column density, in units of Jy sr^{-1} cm^{2} per H atom. We estimate an average column density of hydrogen for RCW175 N(H)$\approx 4.4 \times 10^{22}$ cm^{-22} using the canonical factor 2.13×10^{24} H cm^{-2} per unit of $\tau_{100\mu{\rm m}}$ (Finkbeiner et al. 2004). The best-fitting spinning dust model in Fig. 2 corresponds to N(H)$= 4.4 \times 10^{22}$ cm^{-22}. The observed levels are therefore consistent with the emissivities of Draine & Lazarian (1998b). It is also remarkable that the amplitude of the anomalous component is similar to the emissivity relative to 100 μm observed at high Galactic latitudes (Davies et al. 2006), which is equivalent to 1 Jy at 30 GHz per 6000 Jy at 100 μm. This does not appear to be the case for all HII regions, which have so far shown to have a reduced radio-to-dust emissivity (Dickinson et al. 2007; Scaife et al. 2007). High resolution, multi-frequency data in the range $10-100$ GHz are needed to confirm this result and to investigate the nature of anomalous emission.

5. CONCLUSIONS

Using data from the VSA and CBI, we have observed excess emission at ~ 30 GHz from the HII region RCW175. The flux density spectrum indicates that about half of the flux in this region is from optically thin free-free emission leaving about half unaccounted for. An upper limit at 94 GHz from WMAP data constrains the contribution of thermal dust emission. We have discarded optically thick free-free emission from UC HII regions and GPS sources as possible candidates for this excess; an upper limit at 94 GHz and high resolution radio data rule these out as the primary contributor at ~ 30 GHz. We interpret the excess as electric dipole radiation from small rapidly spinning dust grains as predicted by Draine & Lazarian (1998b). These models provide a reasonable fit to the data that is consistent both in terms of spectral shape and emissivity. High resolution, multi-frequency data in the range $10-100$ GHz are needed to confirm this result and to investigate the nature of anomalous emission.

This work was supported by the Strategic Alliance for the Implementation of New Technologies (SAINT - see www.astro.caltech.edu/chajnantor/saint/index.html) and we are most grateful to the SAINT partners for their strong support. We gratefully acknowledge support from the Kavli Operating Institute and thank B. Rawn and S. Rawn Jr. The CBI was supported by NSF grants 9802989, 0098734 and 0206416, and a Royal Society Small Research Grant. We are particularly indebted to the engineers who maintain and operate the CBI: C. Achermann, R. Bustos, C. Jara, N. Oyarace, R. Reeves, M. Shepherd and C. Verdugo. CD thanks Roberta Paladini and Bill Reach. CD acknowledges support from the U.S. *Planck* project, which is funded by the NASA Science Mission Directorate. SC acknowledges support from FONDECYT grant 1030805, and from the Chilean Center for Astrophysics FONDAP 15010003. AT acknowledges support from Royal Society and STFC research fellowships.

REFERENCES

Altenhoff, W. J., Downes, D., Goad, L., Maxwell, A., & Rinehart, R. 1970, A&AS, 1, 319

Banday, A. J., Dickinson, C., Davies, R. D., Davis, R. J., & Górski, K. M. 2003, MNRAS, 345, 897

Beichman, C. A., Neugebauer, G., Habing, H. J., Clegg, P. E., & Chester, T. J., eds. 1988, Infrared astronomical satellite (IRAS) catalogs and atlases. Volume 1: Explanatory supplement, Vol. 1

Bennett, C. L., Hill, R. S., Hinshaw, G., Nolta, M. R., Odegard, N., Page, L., Spergel, D. N., Weiland, J. L., Wright, E. L., Halpern, M., Jarosik, N., Kogut, A., Limon, M., Meyer, S. S., Tucker, G. S., & Wollack, E. 2003, ApJS, 148, 97

Bonaldi, A., Ricciardi, S., Leach, S., Stivoli, F., Baccigalupi, C., & de Zotti, G. 2007, MNRAS, 382, 1791

Casassus, S., Cabrera, G. F., Förster, F., Pearson, T. J., Readhead, A. C. S., & Dickinson, C. 2006, ApJ, 639, 951

Casassus, S., Nyman, L.-Å., Dickinson, C., & Pearson, T. J. 2007, MNRAS, 382, 1607

Casassus, S., Readhead, A. C. S., Pearson, T. J., Nyman, L.-Å., Shepherd, M. C., & Bronfman, L. 2004, ApJ, 603, 599

Condon, J. J., Cotton, W. D., Greisen, E. W., Yin, Q. F., Perley, R. A., Taylor, G. B., & Broderick, J. J. 1998, AJ, 115, 1693

Davies, R. D., Dickinson, C., Banday, A. J., Jaffe, T. R., Górski, K. M., & Davis, R. J. 2006, MNRAS, 370, 1125

de Oliveira-Costa, A., Tegmark, M., Davies, R. D., Gutiérrez, C. M., Lasenby, A. N., Rebolo, R., & Watson, R. A. 2004, ApJ, 606, L89

Dickinson, C., Battye, R. A., Carreira, P., Cleary, K., Davies, R. D., Davis, R. J., Genova-Santos, R., Grainge, K., Gutiérrez, C. M., Hafez, Y. A., Hobson, M. P., Jones, M. E., Kneissl, R., Lancaster, K., Lasenby, A., Leahy, J. P., Maisinger, K., Ödman, C., Pooley, G., Rajguru, N., Rebolo, R., Rubiño-Martin, J. A., Saunders, R. D. E., Savage, R. S., Scaife, A., Scott, P. F., Slosar, A., Sosa Molina, P., Taylor, A. C., Titterington, D., Waldram, E., Watson, R. A., & Wilkinson, A. 2004, MNRAS, 353, 732

Dickinson, C., Casassus, S., Pineda, J. L., Pearson, T. J., Readhead, A. C. S., & Davies, R. D. 2006, ApJ, 643, L111

Dickinson, C., Davies, R. D., Bronfman, L., Casassus, S., Davis, R. J., Pearson, T. J., Readhead, A. C. S., & Wilkinson, P. N. 2007, MNRAS, 379, 297

Dickinson, C., Davies, R. D., & Davis, R. J. 2003, MNRAS, 341, 369

Draine, B. T. & Lazarian, A. 1998a, ApJ, 494, L19+

—. 1998b, ApJ, 508, 157

—. 1999, ApJ, 512, 740

Dupac, X., Bernard, J.-P., Boudet, N., Giard, M., Lamarre, J.-M., Mény, C., Pajot, F., Ristorcelli, I., Serra, G., Stepnik, B., & Torre, J.-P. 2003, A&A, 404, L11

Fernández-Cerezo, S., Gutiérrez, C. M., Rebolo, R., Watson, R. A., Hoyland, R. J., Hildebrandt, S. R., Rubiño-Martín, J. A., Macías-Pérez, J. F., & Sosa Molina, P. 2006, MNRAS, 370, 15

Finkbeiner, D. P. 2004, ApJ, 614, 186

Finkbeiner, D. P., Langston, G. I., & Minter, A. H. 2004, ApJ, 617, 350

Forbes, D. 1989, A&AS, 77, 439

Gordon, M. A. 1988, ApJ, 331, 509

Handa, T., Sofue, Y., Nakai, N., Hirabayashi, H., & Inoue, M. 1987, PASJ, 39, 709

Haynes, R. F., Caswell, J. L., & Simons, L. W. J. 1978, Australian Journal of Physics Astrophysical Supplement, 45, 1

Hildebrandt, S. R., Rebolo, R., Rubiño-Martín, J. A., Watson, R. A., Gutiérrez, C. M., Hoyland, R. J., & Battistelli, E. S. 2007, MNRAS, 382, 594

Hill, R. S., Weiland, J. L., Odegard, N., Wollack, E., Hinshaw, G., Larson, D., Bennett, C. L., Halpern, M., Page, L., Dunkley, J., Gold, B., Jarosik, N., Kogut, A., Limon, M., Nolta, M. R., Spergel, D. N., Tucker, G. S., & Wright, E. L. 2008, ArXiv e-prints, 803

Hinshaw, G., Weiland, J. L., Hill, R. S., Odegard, N., Larson, D., Bennett, C. L., Dunkley, J., Gold, B., Greason, M. R., Jarosik, N., Komatsu, E., Nolta, M. R., Page, L., Spergel, D. N., Wollack, E., Halpern, M., Kogut, A., Limon, M., Meyer, S. S., Tucker, G. S., & Wright, E. L. 2008, ArXiv e-prints, 803

Langston, G., Minter, A., D'Addario, L., Eberhardt, K., Koski, K., & Zuber, J. 2000, AJ, 119, 2801

Leitch, E. M., Readhead, A. C. S., Pearson, T. J., & Myers, S. T. 1997, ApJ, 486, L23+

Padin, S., Shepherd, M. C., Cartwright, J. K., Keeney, R. G., Mason, B. S., Pearson, T. J., Readhead, A. C. S., Schaal, W. A., Sievers, J., Udomprasert, P. S., Yamasaki, J. K., Holzapfel, W. L., Carlstrom, J. E., Joy, M., Myers, S. T., & Otarola, A. 2002, PASP, 114, 83

Readhead, A. C. S., Mason, B. S., Contaldi, C. R., Pearson, T. J., Bond, J. R., Myers, S. T., Padin, S., Sievers, J. L., Cartwright, J. K., Shepherd, M. C., Pogosyan, D., Prunet, S., Altamirano, P., Bustos, R., Bronfman, L., Casassus, S., Holzapfel, W. L., May, J., Pen, U.-L., Torres, S., & Udomprasert, P. S. 2004, ApJ, 609, 498

Reich, W., Fuerst, E., Reich, P., & Reif, K. 1990, A&AS, 85, 633

Rodgers, A. W., Campbell, C. T., & Whiteoak, J. B. 1960, MNRAS, 121, 103

Rybicki, G. B. & Lightman, A. P. 1979, Radiative processes in astrophysics (New York, Wiley-Interscience, 1979. 393 p.)

Scaife, A., Green, D. A., Battye, R. A., Davies, R. D., Davis, R. J., Dickinson, C., Franzen, T., Génova-Santos, R., Grainge, K., Hafez, Y. A., Hobson, M. P., Lasenby, A., Pooley, G. G., Rajguru, N., Rebolo, R., Rubiño-Martin, J. A., Saunders, R. D. E., Scott, P. F., Titterington, D., Waldram, E., & Watson, R. A. 2007, MNRAS, 377, L69

Scaife, A. M. M., Hurley-Walker, N., Davies, M. L., Duffett-Smith, P. J., Feroz, F., Grainge, K. J. B., Green, D. A., Hobson, M. P., Kaneko, T., Lasenby, A. N., Pooley, G. G., Saunders, R. D. E., Scott, P. F., Titterington, D. J., Waldram, E. M., & Zwart, J. 2008, MNRAS, 385, 809

Sharpless, S. 1959, ApJS, 4, 257

Watson, R. A., Carreira, P., Cleary, K., Davies, R. D., Davis, R. J., Dickinson, C., Grainge, K., Gutiérrez, C. M., Hobson, M. P., Jones, M. E., Kneissl, R., Lasenby, A., Maisinger, K., Pooley, G. G., Rebolo, R., Rubiño-Martin, J. A., Rusholme, B., Saunders, R. D. E., Savage, R., Scott, P. F., Slosar, A., Sosa Molina, P. J., Taylor, A. C., Titterington, D., Waldram, E., & Wilkinson, A. 2003, MNRAS, 341, 1057

Watson, R. A., Rebolo, R., Rubiño-Martín, J. A., Hildebrandt, S., Gutiérrez, C. M., Fernández-Cerezo, S., Hoyland, R. J., & Battistelli, E. S. 2005, ApJ, 624, L89

Wood, D. O. S. & Churchwell, E. 1989, ApJS, 69, 831

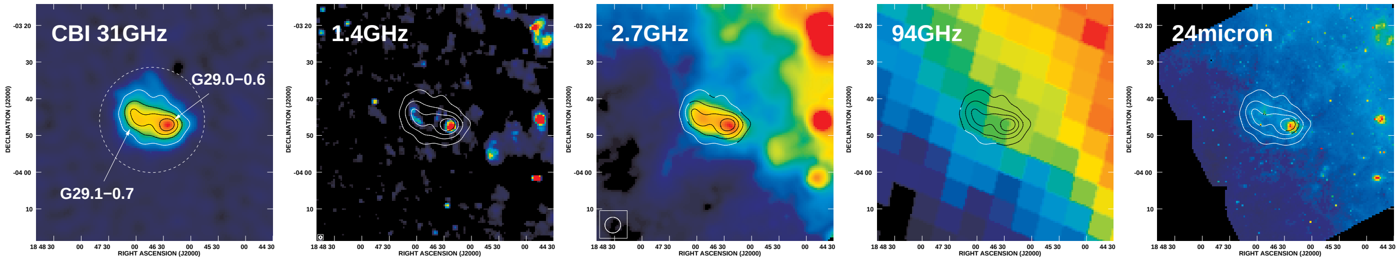

Fig. 1.— Multi-frequency maps of the RCW175 region. From left to right: CBI 31 GHz CLEANed map, NVSS 1.4 GHz, Effelsberg 2.7 GHz, WMAP 94 GHz and *Spitzer* MIPS 24 μm. Angular resolutions and references are given in Table 1. Contours are CBI 31 GHz at $20, 40, 60, 80\%$ of the peak brightness, 1.04 Jy/beam. The CBI primary beam (FWHM) is shown as a dashed line.

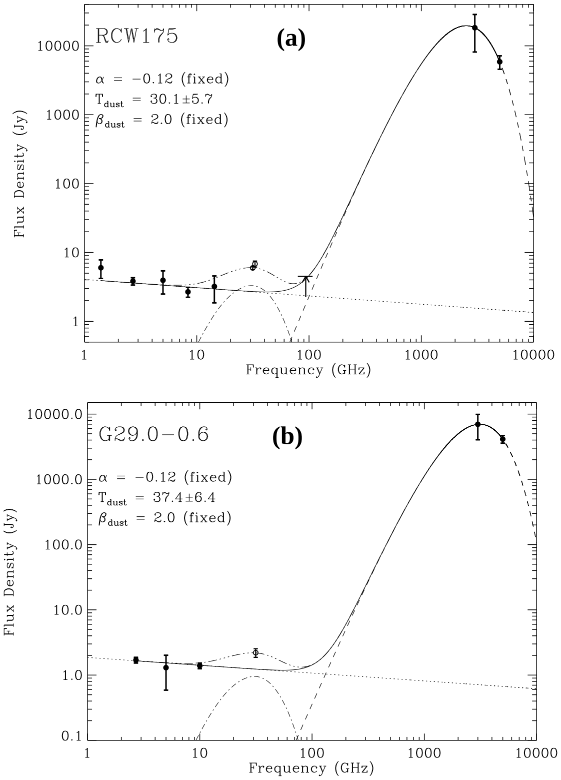

FIG. 2.— Integrated flux density spectrum for a) both components combined (RCW175) and b) the brighter component (G29.0-0.6). Filled circles represent data fitted by a power-law with fixed spectral index (dotted line) and a modified black-body with fixed emissivity (dashed line). The Draine & Lazarian (1998b) CNM spinning dust spectrum (dot-dashed line) has been fitted to the 31/33 GHz data.

TABLE 1
FLUX DENSITIES FOR RCW175 AND G29.0-0.6.

Frequency (GHz)	Telescope/ survey	Angular resolution (arcmin)	Reference for data	Flux density RCW175 (Jy)	Flux density G29.0-0.6 (Jy)
1.4	Green Bank 300 ft	9.4×10.4	Altenhoff et al. (1970)	6.0 ± 1.8	Not resolved
2.7	Effelsberg 100 m	4.3	Reich et al. (1990)	3.83 ± 0.38	1.70 ± 0.17
5	Parkes 64 m	4.1	Haynes et al. (1978)	3.90 ± 0.39	1.30 ± 0.71
8.35	Green Bank 13.7 m	9.7	Langston et al. (2000)	2.68 ± 0.35	Not resolved
10	Nobeyama 45 m	3	Handa et al. (1987)	Not reported	1.39 ± 0.14
14.35	Green Bank 13.7 m	6.6	Langston et al. (2000)	3.21 ± 1.83	Not resolved
31	CBI	4.3×4.0	This work	5.97 ± 0.30	2.20 ± 0.33
33	VSA	13.1×10.0	Todorovic et al. (in prep.)	6.83 ± 0.68	Not resolved
94	WMAP	≈ 12.6	Hinshaw et al. (2008)	< 4.5 (3σ)	< 4.5 (3σ)
2997 (100 μm)	IRAS	≈ 4	Beichman et al. (1988)	18320 ± 10190	6970 ± 2930
4995 (60 μm)	IRAS	≈ 4	Beichman et al. (1988)	5864 ± 1292	4131 ± 548
12875 (24 μm)	*Spitzer* MIPSGAL	0.033	http://irsa.ipac.caltech.edu/	Not fitted	Not fitted